BIOMOLECULES & THERAPEUTICS

Original Article
Biomol Ther 31(6), 674-681 (2023)

Diagnostic Role of Bile Pigment Components in Biliary Tract Cancer

Keun Soo Ahn[1], Koo Jeong Kang[1], Yong Hoon Kim[1], Tae-Seok Kim[1], Kwang Bum Cho[2], Hye Soon Kim[3], Won-Ki Baek[4], Seong-Il Suh[4] and Jin-Yi Han[1,*]

[1]Division of Hepatobiliary and Pancreatic Surgery, Department of Surgery, Keimyung University Dongsan Medical Center, Daegu 42601,
[2]Division of Gaestroenterology, Department of Internal Medicine, Keimyung University Dongsan Medical Center, Daegu 42601,
[3]Division of Endocrinology, Department of Internal Medicine, Keimyung University Dongsan Medical Center, Daegu 42601,
[4]Department of Microbiology, Keimyung University School of Medicine, Daegu 42601, Republic of Korea

Abstract

Bile pigment, bilirubin, and biliverdin concentrations may change as a results of biliary tract cancer (BTC) altering the mechanisms of radical oxidation and heme breakdown. We explored whether changes in bile pigment components could help distinguish BTC from benign biliary illness by evaluating alterations in patients with BTC. We collected bile fluid from 15 patients with a common bile duct stone (CBD group) and 63 individuals with BTC (BTC group). We examined the bile fluid's bilirubin, biliverdin reductase (BVR), heme oxygenase (HO-1), and bacterial taxonomic abundance. Serum bilirubin levels had no impact on the amounts of bile HO-1, BVR, or bilirubin. In comparison to the control group, the BTC group had considerably higher amounts of HO-1, BVR, and bilirubin in the bile. The areas under the curve for the receiver operating characteristic curve analyses of the BVR and HO-1 were 0.832 (p<0.001) and 0.891 (p<0.001), respectively. Firmicutes was the most prevalent phylum in both CBD and BTC, according to a taxonomic abundance analysis, however the Firmicutes/Bacteroidetes ratio was substantially greater in the BTC group than in the CBD group. The findings of this study showed that, regardless of the existence of obstructive jaundice, biliary carcinogenesis impacts heme degradation and bile pigmentation, and that the bile pigment components HO-1, BVR, and bilirubin in bile fluid have a diagnostic significance in BTC. In tissue biopsies for the diagnosis of BTC, particularly for distinguishing BTC from benign biliary strictures, bile pigment components can be used as additional biomarkers.

Key Words: Biliary tract cancers (BTCs), Bile pigment, Heme oxygenase (HO-1), Biliverdin reductase (BVR), Metagenomics

INTRODUCTION

Biliary tract cancers (BTCs), including gallbladder cancer (GBC), ampullary carcinoma (AC), and extra-cholangiocarcinoma (eCCA), are rapidly growing tumors that are usually lethal (de Groen *et al*., 1999; Anderson and Kim, 2009; Javle *et al*., 2016). One of the reasons for this is the lack of biomarkers for early diagnosis. Moreover, differentiating between malignant and benign biliary strictures remains challenging, and invasive endoscopic and percutaneous tissue acquisition have limited diagnostic accuracy (Eloubeidi *et al*., 2004; DeWitt *et al*., 2006). Therefore, novel and reliable biomarkers are required for early diagnosis.

The bile duct plays a crucial role in the formation and secretion of bile, as well as the excretion of circulating xenobiotic substances. In addition to its secretory and excretory functions, the bile duct epithelium plays an important role in the formation of a barrier to the diffusion of toxic substances from the bile into the hepatic interstitial tissue (Rao and Samak, 2013). The main components of bile are water, bile salts, bile pigments, and cholesterol (Boyer, 2013). Bile pigments are endogenous, colored breakdown products of the blood pigment hemoglobin that is excreted in bile (Pimstone *et al*., 1971). The two most important bile pigments are bilirubin, which is orange or yellow, and its oxidized form biliverdin, which is green (Ge, 2015)

Heme is a source of bile pigments. Heme degradation is induced by heme oxygenase (HO)-1 in macrophages of the

Open Access https://doi.org/10.4062/biomolther.2023.010

Received Jan 11, 2023 **Revised** Jun 8, 2023 **Accepted** Jul 4, 2023
Published Online Aug 10, 2023

***Corresponding Author**
E-mail: 407190@ms.kmu.ac.kr
Tel: +82-53-258-7554, Fax: +82-53-258-4710

reticuloendothelial system (RES). HO-1 is a rate-limiting enzyme that catalyzes the conversion of heme to carbon monoxide (CO), free ferrous iron, and biliverdin (Dawn and Bolli, 2005). Biliverdin is rapidly converted to bilirubin by biliverdin reductase (BVR), a molecule with antioxidant properties, and free iron is sequestered by ferritin (Otterbein and Choi, 2000; Ryter *et al*., 2002). Bilirubin moves to the liver through glucuronic acid conjugation and is excreted into the duodenum in bile fluid via the bile duct.

When cancer occurs in the bile duct, the roles of the bile duct epithelium and bile components may be affected. Because CCA arises from the bile duct, bile fluid always directly contacts tumor cells in BTC, and tumor-derived materials might be abundant in bile. In a previous study, we showed that alterations in metabolism and radical oxidation could affect cancer progression, and that bile fluid reflects these alterations in BTC (Ahn *et al*., 2019; Han *et al*., 2020). Thus, heme degradation and bile pigmentation may be affected by cancer, resulting in changes in the concentrations of bilirubin and biliverdin in bile. If so, the levels of HO-1, BVR, and bilirubin in the bile fluid of patients with cancer might be different from those in patients with benign biliary strictures. In addition, these changes may affect bacterial taxonomic abundance in the bile. In this study, we investigated the bile pigment components of patients with BTC to evaluate their diagnostic value.

MATERIALS AND METHODS

Patients

A total of 78 patients were enrolled in the study at Keimyung University Dongsan Hospital between August 2018 and March 2021. Patient characteristics, including age, sex, tumor site, method of obtaining bile, and cancer stage, are shown in Table 1. Bile fluid was obtained from all 78 patients. Sixty-three patients had BTC (BTC group), and 15 patients had common bile duct (CBD) stones and comprised the control group (CBD group). The patients with BTC included 37 men and 26 women, with a mean age of 73.0 ± 9.1 years (range, 45-92 years). After the initial diagnosis of BTC in 63 patients, 32 (50.7%) underwent surgical resection and 31 (49.2%) received palliative chemoradiotherapy or conservative therapy. Cancer stages were determined based on pathologic results (for those who underwent surgical resection) or radiologic findings (for those who did not undergo surgical resection). All procedures were in accordance with the World Medical Association's Declaration of Helsinki (1964, and its later amendments) if they reported on experiments involving human subjects.

Table 1. Clinico-pathological characteristics and stages of patients with BTC and CBD stones

Characteristic	CBD (n=15)	BTC (n=63)	*p*
Age	74.2 ± 13.0	73.0 ± 9.1	0.680
Sex			0.786
- F	5 (33.3%)	26 (41.3%)	
- M	10 (66.7%)	37 (58.7%)	
AJCC Stage			
- I		3 (4.8%)	
- II		13 (20.6%)	
- III		36 (57.1%)	
- IV		11 (17.5%)	
Method of bile collection			
- PTBD	15	50	
- Operation		13	

Bile collection and preparation

Bile samples were collected from 65 patients in both groups through percutaneous transhepatic biliary drainage (PTBD) to relieve cholangitis caused by obstructive jaundice after resolving cholangitis for at least three days after the PTBD procedure. In the remaining 13 patients, bile was collected during surgical resection. The collected bile fluid was immediately centrifuged at 16,000 g for 10 min at 4°C to obtain the supernatant (bile). Each pellet was resuspended in two volumes of chilled phosphate-buffered saline (PBS) and then centrifuged at 16,000 g for 5 min at 4°C to obtain a bile pellet, as described in the protocol by Abi Zabron Imperial College, London, England. All experiments were performed with an Avanti J-25I (Beckman, CA, USA), and bile and pellets were stored at –80°C. After separation, the samples were used in all experiments. This study was approved by the Institutional Review Board of Keimyung University Dongsan Hospital (No. 2018-06-054).

Reagents

Antibodies against HO-1 and BVR were purchased from Abcam (Cambridge, MA, USA). The Bilirubin Direct Gen.2 (BILD2) kit was purchased from Roche (Mannheim, Germany), and the human BVR and HO-1 ELISA Kits were purchased from Biomatik (Cambridge, ON, Canada). Polyvinylidene fluoride (PVDF) membranes were purchased from Amersham (Hybond TM-P: GE Healthcare, Buckinghamshire, UK). Ethanol and all other chemicals were obtained from Sigma (St. Louis, MO, USA).

Bilirubin determination

The amount of bilirubin (direct form) in bile was analyzed using a BILD2 kit (Roche) on a Cobas C502 system (SCL Healthcare) by SCL Healthcare (Yongin, Korea).

Measurement of HO-1 and BVR activity

BVR and HO-1 activity levels in bile were quantified using an ELISA kit, according to the manufacturer's instructions. Briefly, 100 μL bile (1:10 dilution) and two-fold serial dilutions of each standard were dispensed into microplate wells precoated with the capture antibody. For the measurements, 100 μL of bile μL was added to each well of the microplate and incubated at 37°C for 60-90 min. After incubation, we removed the bile, added 100 μL of biotinylated antibody working solution and detector antibody to each well, and incubated the plate at 37°C for 60 min. After washing, the plate was incubated with streptavidin-horseradish peroxidase (HRP) conjugate at 37°C for 30 min, developed with 90 μL of 3,3',5,5'-tetramethylbenzidine (TMB) substrate at 37°C in the dark for 10-20 min, and stopped by adding 50 μL of stop solution to each well. Absorbance was read at 450 nm using an Infinite M 200 Pro multifunction microplate reader (TECAN, Männedorf, Switzerland), and BVR and HO-1 concentrations were calculated based on a standard curve and expressed as ng of standard concentration/mg of protein. Protein concentrations in bile were determined by the Bradford method (Pierce, Rockford, IL, USA)

using bovine serum albumin (BSA) as a standard.

Western analysis for HO-1 and BVR

Total proteins were extracted using RIPA lysis buffer (Cat. #MB-030-0050, Rockland, Limerick, ME, USA) containing protease inhibitor cocktail (Cat. #PPI1015, Quartett, Berlin, Germany). 10 μg total proteins were subjected to sodium dodecyl sulfate-polyacrylamide gel electrophoresis and then proteins were transferred to nitrocellulose membrane using the Trans-Blot Turbo Transfer System (Bio-Rad, Hercules, CA, USA). The membranes were blocked with Tris-buffered saline containing 5% skim milk (Bio-Rad) and 0.2% Tween 20 (Bio-Rad). The following primary antibodies were used: HO-1 and BVR (1:500, Abcam, ab68477, ab192925) and GAPDH (1:2000, Cell Signaling Technology, #2118, Danvers, MA, USA). After reaction with horseradish peroxidase conjugated secondary antibodies (Santa Cruz Biotechnology Inc., Dallas, TX, USA) bands on the membranes were visualized by Clarity western ECL substrate chemiluminescent (Bio-Rad) following the manufacturer's suggested procedure. The densitometry of the bands was determined using a chem-Doc XRS+ imaging system (Bio-Rad) and normalized to GAPDH, which served as the loading control.

DNA extraction and sequencing

DNA was extracted from 1 mL of bile using a DNeasy Power Soil Kit (Qiagen, Hilden, Germany) according to the manufacturer's instructions. Extracted DNA was quantified using Quant-IT Pico Green (Invitrogen, Waltham, MA, USA). Sequencing libraries were prepared according to the Illumina 16S metagenomic sequencing library protocols to amplify the V3 and V4 regions. A 2-ng amount of gDNA was used for PCR amplification with 5x reaction buffer, 1 mM dNTP mix, 500 nM universal F/R PCR primer, and Herculase II fusion DNA polymerase (Agilent Technologies, Santa Clara, CA, USA). The cycling conditions for the first PCR were as follows: 3 min at 95°C for heat activation, 25 cycles of 30 s at 95°C, 30 s at 55°C, and 30 s at 72°C, followed by a 5-min final extension at 72°C. The universal primer pair with Illumina adapter overhang sequences used for the first amplification was:

V3-F: 5'-TCGTCGGCAGCGTCAGATGTGTATAAGAGACAGCCTACGGGNGGCWGCAG-3'
V4-R: 5'-GTCTCGTGGGCTCGGAGATGTGTATAAGAGACAGGACTACHVGGGTATCTAATCC-3'

The first PCR product was purified with AMPure beads (Agencourt Bioscience, Beverly, MA, USA). Following the purification, 2 μL of the first PCR product was amplified for final library construction containing the index using Nextera XT Indexed Primer. The cycle conditions for the second PCR were the same as those forr first PCR, except that only ten cycles were used. The PCR products were purified using AMPure beads. The final purified product was quantified using quantitative PCR (qPCR) according to the qPCR Quantification Protocol guide (KAPA Library Quantification kit for Illumina Sequencing platforms) and qualified using the Tape Station D1000 Screen Tape (Agilent Technologies, Waldbronn, Germany). Paired end (2×300 bp) sequencing was performed by Macrogen (Seoul, Korea) using the MiSeq™ platform (Illumina, San Diego, CA, USA)

Amplicon sequence variants (ASVs) analysis

After sequencing was completed, the Illumina Miseq raw data were classified by sample using an index sequence, and a paired-end FASTQ file was created for each sample. The sequencing adapter sequence and F/R primer sequence of the target gene region were removed using Cutadapt (v3.2) (Martin, 2011). For error correction of the amplicon sequencing process, the DADA2 (v1.18.0) (Callahan *et al*., 2016) and package of the R (v4.0.3) program was used. For paired end reads, the forward sequence (Read1) and reverse sequence (Read2) were cut to 250 bp and 200 bp, respectively, and sequences with expected errors of two or more were excluded. An error model was then established for each batch to remove noise from each sample. After assembling the paired-end sequences corrected for sequencing errors into one sequence, the chimeric sequence was removed using the DADA2 consensus method to form amplicon sequence variants (ASVs). For comparative analysis of the microbial community, the QIIME (v1.9) (Caporaso *et al*., 2010) program was used for normalization by applying subsampling based on the number of reads of the sample with the minimum number of reads among all samples. For each ASV sequence, BLAST+ (v2.9.0) (Camacho *et al*., 2008) was performed using the reference database (NCBI 16S Microbial DB), and taxonomic information for the organism of the subject with the highest similarity was assigned.

Statistical analysis

Data analysis was conducted using R (http//www.r-project.org) and Simplot (SysTest Software Inc., Palo Alto, CA, USA). The cutoff value foe individual values was based on the receiver operating characteristic (ROC) curve. Continuous values are expressed as mean ± SD. For comparisons between two groups, an independent *t*-test was used for continuous variables, and a χ^2 test was used for categorical variables. A significance was ser at $p<0.05$.

RESULTS

Demographic characteristics of the study population

The mean age of the study population was 74.0 ± 11.1 years and with 31 females and 47 males. There were no statistically significant differences in age or sex between the CBD and BTC groups. In the BTC group, 74.6% of the patients were in an advanced stage, higher than the American Joint Committee on Cancer (AJCC) stage III (Table 1).

Correlation analysis of bile HO-1, BVR, and bilirubin with serum bilirubin

Correlation analysis was performed to assess whether bile HO-1, BVR, and bilirubin levels were associated with serum bilirubin levels. The Pearson's correlation coefficient between serum bilirubin and the three markers in bile was very low with no statistical significance (Fig. 1). Therefore, bile HO-1, BVR, and bilirubin levels were not affected by serum bilirubin levels.

Expression level of HMOX1 and BLVRA in cancer tissues

In many cancers, expression of HMOX1 (RNA of HO-1) and BLVRA (RNA of BVR) are variable. In BTC, expression level of BLVRA is significantly higher than normal adjacent liver tissue (Supplementary Fig. 1, 2) (Farshidfar *et al*., 2017; Ahn *et*

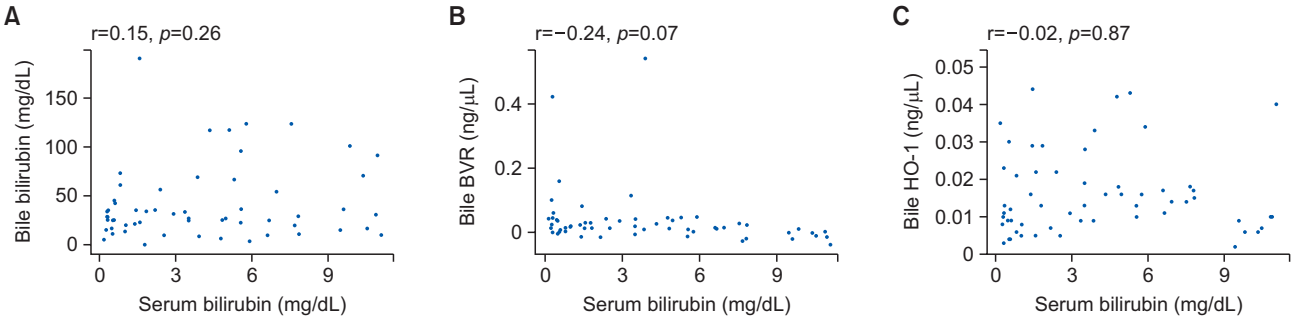

Fig. 1. Correlation between serum and bile bilirubin levels (A), serum bilirubin and bile BVR (B), and serum bilirubin and bile HO-1 (C).

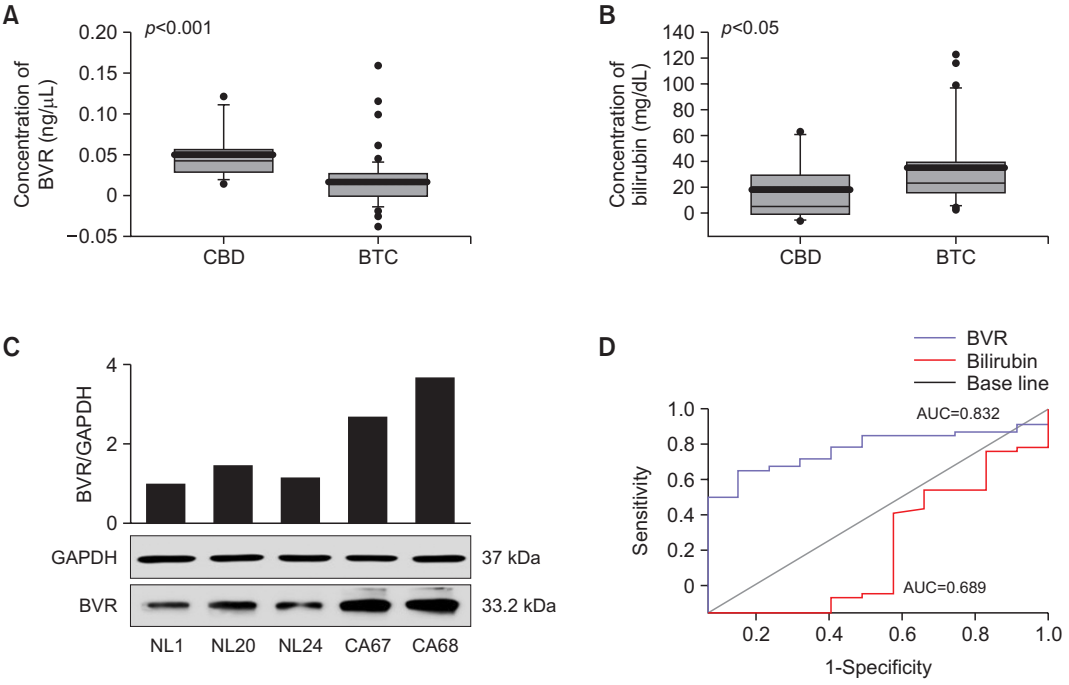

Fig. 2. Comparative changes in BVR and bilirubin levels in the bile of patients with CBD stones and BTC. (A) BVR activity. (B) Bilirubin level. The number of patients in each group was indicated as follows. BVR activity (CBD, n=14, BTC, n=56), Bilirubin level (CBD, n=11, BTC n=53). (C) Protein level and relative expression of BVR. (D) ROC analysis of BVR and bilirubin. GAPDH levels were measured to confirm equal protein loading. Patients were in two groups (n=11–56/group). All data are presented as means ± SD.

al., 2019).

Comparative changes in BVR and bilirubin amounts in patients with bile CBD stones and BTC

Biliverdin and bilirubin, the principal bile pigments, are the end-products of heme catabolism. To identify the component ratios, we investigated the activity of BVR and amount of bilirubin in the bile of the CBD and BTC groups. BVR activity was significantly decreased in bile in the BTC group compared to that the CBD group (0.033 ± 0.091, 0.050 ± 0.030 ng/μg protein; p<0.001; Fig. 2A) and the amount of the direct form of bilirubin was significantly increased in the BTC group compared that in the CBD group (42.6 ± 37.4, 23.0 ± 22.5 ng/mL; p=0.05; Fig. 2B). The expression of BVR in the bile of the BTC group was 2- or 3-fold higher than that in the CBD group (Fig. 2C). ROC curve analysis was performed to evaluate the predictive ability of each parameter for BTC diagnosis. In the ROC analysis of the BVR, the area under the curve (AUC) was 0.832 (0.736-0.928; p<0.001; Fig. 2D), and the optimal cut-off value for BVR activity was 0.023 ng/mg protein, with a sensitivity of 69.0% and specificity of 92.9%. However, the diagnostic power of bilirubin was lower than that of BVR (AUC: 0.689; Fig. 2D).

Classification of bile pigments in the bile of patients with CBD stones and BTC

Since bile color is determined by the BVR and bilirubin components in bile, bile color can be differentiated in the BTC and CBD groups. Bile pigments are largely classified into three colors, green, brown, and black, as shown in Fig. 3. In patients in the CBD stone group, brown-black color was more frequent than green. However, BVR, bilirubin, and HO-1 levels did not

differ according to bile color (Table 2).

Alterations in HO-1 in bile in patients with CBD stones and BTC

To identify the possible mechanism of degradation, we estimated the activity of HO-1 using ELISA. HO-1 Activity was significantly lower in the BTC group than in the CBD group, as shown in Fig. 4A (0.012 ± 0.007 and 0.036 ± 0.017 ng/μg protein; $p<0.001$). In addition to HO-1 activity, we analyzed the relative expression of HO-1; and found a 2- or 3-fold increase in the BTC group compared to the CBD group (Fig. 4B). In the ROC analysis of HO-1, the AUC was 0.891 (0.789-0.993; $p<0.001$). The optimal cut-off value was 0.019 ng/mg protein, with a sensitivity of 87.7% and specificity of 78.6% (Fig. 4C). These data suggest that heme degradation may be accelerated through HO-1 upregulation in patients with BTC compared with that in patients with CBD stones.

Taxonomic abundance at the phylum level in the bile of patients with CBD stones and BTC

For bile microbiome profiling in the two groups, we compared the taxonomic compositions obtained for V3V4 analysis. There was an average of 215.28 raw reads in the BTC group and 224.31 in the CBD group. After 30% quality filtering, an average of 81.57 and 81.76 and high-quality 16S rRNA sequences were obtained. In the statistical analysis, refers to the number of unique ASVs in each group (observed species index). Chao1, Shannon, and Gini-Simpson indices, including ASVs, are all alpha-diversity indices The Wilcoxon rank-sum test was used to identify differences between the two groups (Bauer, 1972). The differences in ASVs between the CBD and BTC groups were not significant ($p=0.48$), with an average of 175 ASVs in the CBD group and 159.16 in the BTC group (Fig. 5A). Differences in the Chao1, Shannon, and Gini-Simpson indices were also not significant ($p=0.48$, 0.61, and 1, respectively) with averages in the CBD group of 175, 3.59, and 0.71, and 159.1, 3.25, and 0.13, respectively, in the BTC group (Fig. 5B-5D).

Based on the assigned taxonomic analysis, we profiled relative phylum abundance using stacked bar plots (Fig. 6). *Firmicutes* was the predominant phylum, contributing 51.56% and 39.04% of the bile microbiota in the BTC and CBD groups, respectively, followed by *Bacteroidetes*, which contributed 9.32% and 7.37%, respectively. Although *Firmicutes* was the most abundant phylum in both the CBD and BTC groups, it was significantly more abundant in the BTC group than in the CBD group. In addition, the *Firmicutes/Bacteroidetes* ratio was significantly higher in the BTC group than in the CBD group (Fig. 6A) and the *Verrucomicrobia / Proteobacteria* ratio was higher in the CBD group than in the BTC group. Interestingly, in the sub-analysis according to bile color, *Proteobacteria* were abundant in green color, especially in the CBD group (Fig. 6B). In brown-black colored bile, the ratio of *Bacteroidetes* was very low, especially in the BTC group (Fig. 6C).

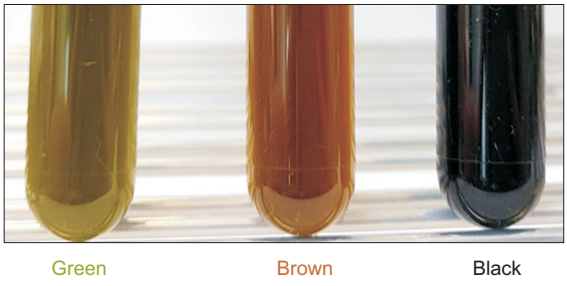

Fig. 3. Classification of bile pigments in the bile of patients with CBD stones and BTC. The three bile pigment colors.

DISCUSSION

A few studies have reported alterations in bile acid components and concentrations in the bile of patients with BTC, and the total bile acid and conjugated bile acid concentrations were higher in patients with BTC than in those with benign biliary disease. However, those parameters were affected by

Table 2. Color differentiation in the bile of patients with CBD stones and BTC

	Green (n=21)	Brown – black (n=52)	*p*
CBD/BTC	3/18	12/40	<0.001
BVR	0.017 ± 0.020 (18)	0.019 ± 0.037 (35)	0.831
Bilirubin	31.1 ± 13.9 (17)	45.3 ± 12.9 (35)	0.08
HO-1	0.013 ± 0.006 (17)	0.011 ± 0.0306 (35)	0.162

Color could not be determined in five patients.

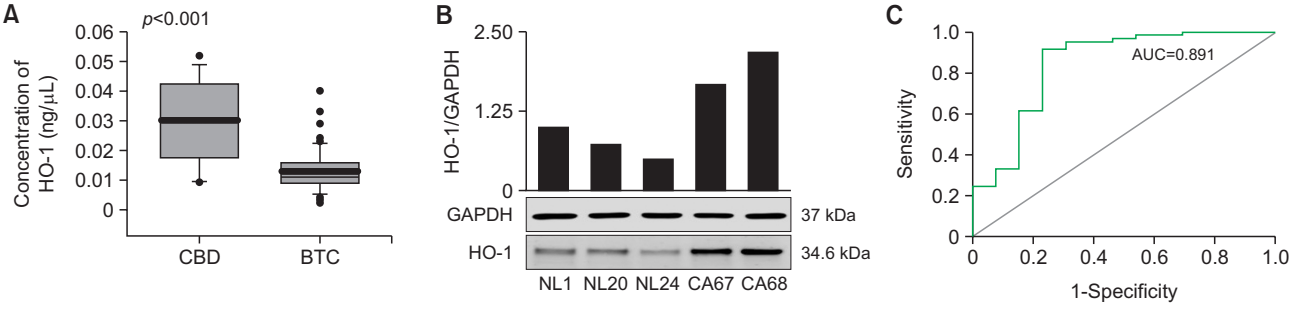

Fig. 4. HO-1 regulation in the bile of patients with CBD stones and BTC. (A) HO-1 activity. The number of patients in each group was indicated as follows (CBD, n=13, BTC, n=57). (B) Protein level and relative expression. (C) ROC analysis of HO-1. GAPDH levels were measured to confirm equal protein loading. Patients were in two groups (n=13–57/group). All data are presented as means ± SD.

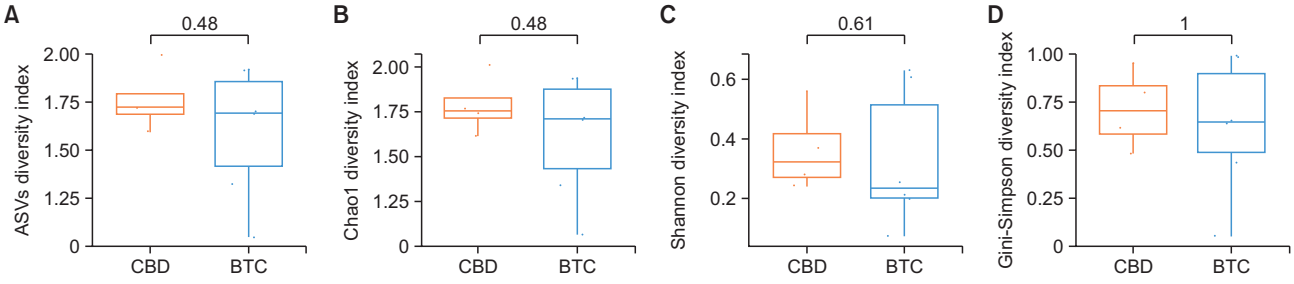

Fig. 5. Alpha-diversity at the phylum level in the bile of patients with CBD stones and BTC (CBD, n=4, BTC, n=6). (A) ASVs diversity index of bile in the CBD and BTC. (B) Chao1 diversity index of bile in the CBD and BTC. (C) Shannon diversity index of bile in the CBD and BTC. (D) Gini Simpson diversity index of bile in the CBD and BTC.

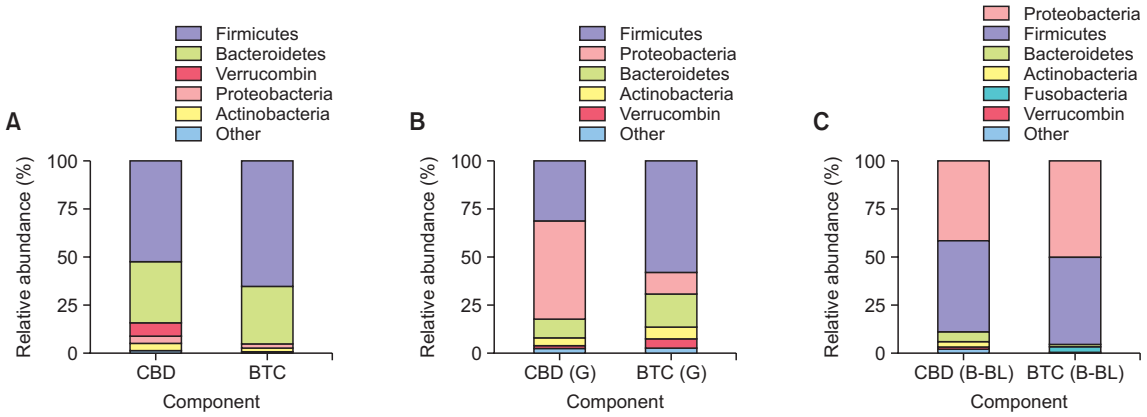

Fig. 6. Taxonomic abundance at the phylum level in the bile of patients with CBD stones and BTC (CBD, n=4, BTC, n=6). (A) Relative abundance of bile in the CBD and BTC groups. (B) Relative abundance of bile in the CBD and BTC groups with green color. (C) Relative abundance of bile in the CBD and BTC groups with brown-black color.

serum bilirubin levels, high concentrations of bile acid in high serum bilirubin conditions, and the bile pigment components changed frequently due to bile duct obstruction. Therefore, bile acid concentrations might be dependent on the degree of bile duct obstruction, and its diagnostic value is limited, especially in patients with non-obstructive jaundice in BTC (Jusakul *et al*., 2012). However, the present study showed elevated expression of HO-1, BVR, and bilirubin in the bile of BTC (decreased HO-1 and BVR activity). These parameters were not affected by serum bilirubin levels (Fig. 1). They are involved in heme metabolism and interact with one another during this process. Our study demonstrated that biliary HO-1, BVR, and bilirubin levels have diagnostic roles in BTC, regardless of the presence of obstructive jaundice. Although a few studies have suggested a role for HO-1 and BVR in cancer, they were found in cancer tissues rather than in bile fluid. This is the first study to reveal the diagnostic value of HO-1 and BVR in bile. It suggests that bile fluid represents the oncogenic characteristics of BTC tissues. Since the role of a tissue biopsy in BTC is limited and it is an invasive procedure, measuring HO-1, BVR, and bilirubin in bile might serve as a biomarker for diagnosing BTC, either alone or as a supplement to tissue biopsy in BTC and especially, in differentiating BTC from benign biliary stricture.

HO-1 metabolizes heme to biliverdin, bilirubin, carbon monoxide, and ferrous iron, and has cytoprotective effects against stress. Therefore, HO-1 expression is highly induced under oxidative stress conditions. HO-1 is also elevated in many cancer tissues and is related to its accommodation in the tumor microenvironment for cancer cell growth, angiogenesis, and metastasis (Nitti *et al*., 2017; Chiang *et al*., 2018). HO-1 overexpression protects against the anti-tumor activity of chemotherapeutic agents (Jeon *et al*., 2012; Yin *et al*., 2012). In contrast, the high expression of HO-1 in tumor cells plays a role in cancer protection by; enhancing cell death by inducing ferroptosis through iron accumulation (Chang *et al*., 2018). Since elevated HO-1 expression in cancer can be a consequence of elevated BVR levels, BVR is usually overexpressed in cancer cells (Maines *et al*., 1999). Like to HO-1, elevated BCR levels in cancer cells are related to responses to cancer-related hypoxia (Gibbs *et al*., 2010; Kim *et al*., 2013). Although BVR is a cytoprotective protein like to HO-1, BVR acts as a promotor of carcinogenesis and tumor progression by modulating the Ras-MAPK and PI3K/Akt pathways (Malumbres and Barbacid, 2003; Gibbs *et al*., 2015). Meanwhile, bilirubin levels in bile were higher in the BTC group than in the CBD group as a consequence of elevated HO-1 and BVR. Usually, serum bilirubin levels in periampullary cancer are higher than those in benign strictures or choledocholithiasis, and this may be caused by changes in the bile salt composition (Jusakul *et al*., 2012; Krupa *et al*., 2021). However, since serum bilirubin levels are highly dependent on the period of biliary obstruc-

tion, they cannot be used as a screening test for predicting whether the obstruction is likely to be malignant or benign. Bile bilirubin levels are regulated by the upstream processes of HO-1, BVR, and other consequent signaling pathways during carcinogenesis, so measuring bilirubin in bile is more helpful than serum bilirubin in differentiating the cause of obstructive jaundice.

Bilirubin, which is brown, black in color, and biliverdin, which is green in color, are the two main types of bile pigments. The differences in color and pigment components were consistent with heme degradation, and pigment color appeared to be reflected by the bile pigment component ratio. Although our results indicated that changes in BVR and bilirubin were related to differences in color in the BTC group (Table 2), they were not statistically significant. Bile color is determined by a combination of bile pigments, and it is difficult to define a wide spectrum of colors by subjective observation. The results in Fig. 6 suggest that the microbiota composition is also important for bile color.

In the microbiota composition analysis of bile, *Firmicutes*, which are associated with the mucosa in colon cancer, were significantly more abundant in the BTC group than in the CBD group, whereas *Proteobacteria*, which are less abundant in colon cancer (Gao *et al*., 2015), were significantly more abundant in the CBD group (Fig. 5A). Interestingly, the dominant phyla and ratios were different not only based on tumor or benign lesions but also on bile color. Although microbiota was analyzed only in a portion of the study population, the results indicated that taxonomic abundance may play distinct functional roles in the bile environment and is associated with cancer cells, as well as bile pigments, inflammation (cholangitis), and other factors that promote interactions between the bacteria and cancerous conditions. Changes in heme degradation and bile pigment composition in patients with BTC may affect the microbiota and require further study.

Since BVR acts as a promoter of carcinogenesis and tumor progression by modulating Ras-MAPK and PI3K/AKT pathways, regulating the activity of BVR can be a potential approach to treatment of BTC. A recent study showed that BVR-based peptides that inhibit its activity negatively affect growth-promoting functions in cancer cell lines (Gibbs *et al*., 2015). Inhibition of HO-1 could enhance chemosensitivity and suppress the proliferation of pancreatic cancer cell lines (Han *et al*., 2018). Therefore, bile pigment components offer a novel approach to the treatment of BTC, as well as a diagnostic marker.

In this paper, we investigated the effect of the bile pigment component on carcinogenesis. However, we could not show the molecular mechanism of bile pigment components in BTC, and it can be a limitation of this study. There have been a few studies on the effects of BVR and HO-1 on carcinogenesis in cholangiocarcinoma tissue, and the purpose of this study was performed with the purpose of showing that these phenomena in bile duct cancer tissue can also be shown through bile fluid. In addition, this study was performed in single institution with small case numbers, and further validation with other cohorts is necessary.

In conclusion, this study demonstrated that biliary carcinogenesis affects heme degradation and bile pigmentation and that the components of bile pigment, HO-1, BVR, and bilirubin in bile fluid have a diagnostic role in BTC, regardless of the presence of obstructive jaundice. They have a role as biomarkers for diagnosing BTC, either alone or as an auxiliary tool to tissue biopsy in BTC and especially, in differentiating BTC from benign biliary stricture.

CONFLICT OF INTEREST

The authors declare no conflict of interest.

ACKNOWLEDGMENTS

In this study, the bile fluids were collected by Sung-Mi Pyo, Seo-Yeon Cha, and So-Jeong Kim. The biospecimens and data used in this study were provided by the Keimyung University Dongsan Hospital Biobank, which is a member of the Korea Biobank Network. This work was supported by the Priority Research Centers Program through the National Research Foundation of Korea (NRF) funded by the Ministry of Education, Science and Technology (NRF-2022 R1A2C4001769).

REFERENCES

Ahn, K. S., O'Brien, D., Kang, Y. N., Mounajjed, T., Kim, Y. H., Kim, T. S., Kocher, J. A., Allotey, L. K., Borad, M. J., Roberts, L. R. and Kang, K. J. (2019) Prognostic subclass of intrahepatic cholangiocarcinoma by integrative molecular-clinical analysis and potential targeted approach. *Hepatol. Int.* **13**, 490-500.

Anderson, C. and Kim, R. (2009) Adjuvant therapy for resected extrahepatic cholangiocarcinoma: a review of the literature and future directions. *Cancer Treat. Rev.* **35**, 322-327.

Bauer, D. F. (1972) Constructing confidence sets using rank statistics. *J. Am. Stat. Assoc.* **67**, 687-690.

Boyer, J. L. (2013) Bile formation and secretion. *Compr. Physiol.* **3**, 1035-1078.

Callahan, B. J., McMurdie, P. J., Rosen, M. J., Han, A. W., Johnson, A. J. and Holmes, S. P. (2016) DADA2: high-resolution sample inference from Illumina amplicon data. *Nat. Methods* **13**, 581-583.

Camacho, C., Coulouris, G., Avagyan, V., Ma, N., Papadopoulos, J., Bealer, K. and Madden, T. L. (2008) BLAST+: architecture and applications. *BMC Bioinformatics* **10**, 421.

Caporaso, J. G., Kuczynski, J., Stombaugh, J., Bittinger, K., Bushman, F. D., Costello, E. K., Fierer, N., Pena, A. G., Goodrich, J. K., Gordon, J. I., Huttley, G. A., Kelley, S. T., Knights, D., Koenig, J. E., Ley, R. E., Lozupone, C. A., McDonald, D., Muegge, B. D., Pirrung, M., Reeder, J., Sevinsky, J. R., Turnbaugh, P. J., Walters, W. A., Widmann, J., Yatsunenko, T., Zaneveld, J. and Knight, R. (2010) QIIME allows analysis of high-throughput community sequencing data. *Nat. Methods* **7**, 335-336.

Chang, L. C., Chiang, S. K., Chen, S. E., Yu, Y. L., Chou, R. H. and Chang, W. C. (2018) Heme oxygenase-1 mediates BAY 11-7085 induced ferroptosis. *Cancer Lett.* **416**, 124-137.

Chiang, S. K., Chen, S. E. and Chang, L. C. (2018) A dual role of heme oxygenase-1 in cancer cells. *Int. J. Mol. Sci.* **20**, 39.

Dawn, B. and Bolli, R. (2005) HO-1 induction by HIF-1: a new mechanism for delayed cardioprotection? *Am. J. Physiol. Heart Circ. Physiol.* **289**, H522-H524.

de Groen, P. C., Gores, G. J., LaRusso, N. F., Gunderson, L. L. and Nagorney, D. M. (1999) Biliary tract cancers. *N. Engl. J. Med.* **341**, 1368-1378.

DeWitt, J., Misra, V. L., Leblanc, J. K., McHenry, L. and Sherman, S. (2006) EUS-guided FNA of proximal biliary strictures after negative ERCP brush cytology results. *Gastrointest. Endosc.* **64**, 325-333.

Eloubeidi, M. A., Chen, V. K., Jhala, N. C., Eltoum, I. E., Jhala, D., Chhieng, D. C., Syed, S. A., Vickers, S. M. and Mel Wilcox, C. (2004) Endoscopic ultrasound-guided fine needle aspiration biopsy of suspected cholangiocarcinoma. *Clin. Gastroenterol. Hepatol.* **2**,

209-213.
Farshidfar, F., Zheng, S., Gingras, M. C., Newton, Y., Shih, J., Robertson, A. G., Hinoue, T., Hoadley, K. A., Gibb, E. A., Roszik, J., Covington, K. R., Wu, C. C., Shinbrot, E., Stransky, N., Hegde, A., Yang, J. D., Reznik, E., Sadeghi, S., Pedamallu, C. S., Ojesina, A. I., Hess, J. M., Auman, J. T., Rhie, S. K., Bowlby, R., Borad, M. J., Zhu, A. X., Stuart, J. M., Sander, C., Akbani, R., Cherniack, A. D., Deshpande, V., Mounajjed, T., Foo, W. C., Torbenson, M. S., Kleiner, D. E., Laird, P. W., Wheeler, D. A., McRee, A. J., Bathe, O. F., Andersen, J. B., Bardeesy, N., Roberts, L. R. and Kwong, L. N. (2017) Integrative genomic analysis of cholangiocarcinoma identifies distinct IDH-mutant molecular profiles. *Cell Rep.* **18**, 2780-2794.
Gao, Z., Guo, B., Gao, R., Zhu, Q. and Qin, H. (2015) Microbiota disbiosis is associated with colorectal cancer. *Front. Microbiol.* **6**, 20.
Ge, O. (2015) Pigments and minerals. In Essentials of Medical Biochemistry.
Gibbs, P. E., Miralem, T. and Maines, M. D. (2010) Characterization of the human biliverdin reductase gene structure and regulatory elements: promoter activity is enhanced by hypoxia and suppressed by TNF-alpha-activated NF-kappaB. *FASEB J.* **24**, 3239-3254.
Gibbs, P. E., Miralem, T. and Maines, M. D. (2015) Biliverdin reductase: a target for cancer therapy? *Front. Pharmacol.* **6**, 119.
Han, J. Y., Ahn, K. S., Baek, W. K., Suh, S. I., Kim, Y. H., Kim, T. S. and Kang, K. J. (2020) Usefulness of bile as a biomarker via ferroptosis and cysteine prenylation in cholangiocarcinoma; role of diagnosis and differentiation from benign biliary disease. *Surg. Oncol.* **34**, 174-181.
Han, L., Jiang, J., Ma, Q., Wu, Z. and Wang, Z. (2018) The inhibition of heme oxygenase-1 enhances the chemosensitivity and suppresses the proliferation of pancreatic cancer cells through the SHH signaling pathway. *Int. J. Oncol.* **52**, 2101-2109.
Javle, M., Bekaii-Saab, T., Jain, A., Wang, Y., Kelley, R. K., Wang, K., Kang, H. C., Catenacci, D., Ali, S., Krishnan, S., Ahn, D., Bocobo, A. G., Zuo, M., Kaseb, A., Miller, V., Stephens, P. J., Meric-Bernstam, F., Shroff, R. and Ross, J. (2016) Biliary cancer: utility of next-generation sequencing for clinical management. *Cancer* **122**, 3838-3847.
Jeon, W. K., Hong, H. Y., Seo, W. C., Lim, K. H., Lee, H. Y., Kim, W. J., Song, S. Y. and Kim, B. C. (2012) Smad7 sensitizes A549 lung cancer cells to cisplatin-induced apoptosis through heme oxygenase-1 inhibition. *Biochem. Biophys. Res. Commun.* **420**, 288-292.
Jusakul, A., Khuntikeo, N., Haigh, W. G., Kuver, R., Ioannou, G. N., Loilome, W., Namwat, N., Bhudhisawasdi, V., Pugkhem, A., Pairojkul, C. and Yongvanit, P. (2012) Identification of biliary bile acids in patients with benign biliary diseases, hepatocellular carcinoma and cholangiocarcinoma. *Asian Pac. J. Cancer Prev.* **13 Suppl**, 77-82.
Kim, S. S., Seong, S., Lim, S. H. and Kim, S. Y. (2013) Biliverdin reductase plays a crucial role in hypoxia-induced chemoresistance in human glioblastoma. *Biochem. Biophys. Res. Commun.* **440**, 658-663.
Krupa, L., Staron, R., Dulko, D., Lozinska, N., Mackie, A. R., Rigby, N. M., Macierzanka, A., Markiewicz, A. and Jungnickel, C. (2021) Importance of bile composition for diagnosis of biliary obstructions. *Molecules* **26**, 7279.
Maines, M. D., Mayer, R. D., Erturk, E., Huang, T. J. and Disantagnese, A. (1999) The oxidoreductase, biliverdin reductase, is induced in human renal carcinoma--pH and cofactor-specific increase in activity. *J. Urol.* **162**, 1467-1472.
Malumbres, M. and Barbacid, M. (2003) RAS oncogenes: the first 30 years. *Nat. Rev. Cancer* **3**, 459-465.
Martin, M. (2011) Cutadapt removes adapter sequences from high-throughput sequencing reads. *EMBnet J.* **17**, 10-12.
Nitti, M., Piras, S., Marinari, U. M., Moretta, L., Pronzato, M. A. and Furfaro, A. L. (2017) HO-1 induction in cancer progression: a matter of cell adaptation. *Antioxidants (Basel)* **6**, 29.
Otterbein, L. E. and Choi, A. M. (2000) Heme oxygenase: colors of defense against cellular stress. *Am. J. Physiol. Lung Cell. Mol. Physiol.* **279**, L1029-L1037.
Pimstone, N. R., Tenhunen, R., Seitz, P. T., Marver, H. S. and Schmid, R. (1971) The enzymatic degradation of hemoglobin to bile pigments by macrophages. *J. Exp. Med.* **133**, 1264-1281.
Rao, R. K. and Samak, G. (2013) Bile duct epithelial tight junctions and barrier function. *Tissue Barriers* **1**, e25718.
Ryter, S. W., Otterbein, L. E., Morse, D. and Choi, A. M. (2002) Heme oxygenase/carbon monoxide signaling pathways: regulation and functional significance. *Mol. Cell. Biochem.* **234-235**, 249-263.
Yin, Y., Liu, Q., Wang, B., Chen, G., Xu, L. and Zhou, H. (2012) Expression and function of heme oxygenase-1 in human gastric cancer. *Exp. Biol. Med. (Maywood)* **237**, 362-371.